Fusion Engineering and Design 219 (2025) 115297

Contents lists available at ScienceDirect

Fusion Engineering and Design

journal homepage: www.elsevier.com/locate/fusengdes

ITER-relevant experimental neutronic activities at JET during DTE3 and at the Frascati neutron generator

N. Fonnesu [a,*], P. Beaumont [b], T. Berry [b], A. Colangeli [a], F. Dacquait [c], M. Damiano [d], D. Flammini [a], C.L. Grove [b], X. Litaudon [c], S. Loreti [a], M. Lungaroni [a], S. Mianowski [b], F. Moro [a], S. Noce [a], J. Peric [e], A. Previti [a], V. Radulović [e], R. Villari [a], P. Zito [a], JET Contributors[1]

[a] ENEA, Nuclear Department, Via E. Fermi 45 00044 Frascati, Rome, Italy
[b] United Kingdom Atomic Energy Authority, Culham Science Centre, Abingdon OX14 3DB, UK
[c] CEA, Cadarache F-13108St-Paul-Lez-Durance, France
[d] University of Rome "Tor Vergata", Industrial Engineering Department, Via del Politecnico 1 00133, Rome, Italy
[e] Reactor Physics Department, Jožef Stefan Institute, Jamova cesta 39 1000 Ljubljana, Slovenia

ARTICLE INFO

Keywords:
JET
ITER
FNG
ACP
SDDR
TBMD
GENeuSIS
Shutdown dose rate
Water activation
Activation corrosion products

ABSTRACT

The technological exploitation of deuterium-tritium (DT) campaigns at JET under EUROfusion work package PrIO (Preparation of ITER Operations) aimed at taking advantage of the ITER-relevant radiation fields to improve the knowledge of nuclear technology and safety and to develop and validate nuclear codes, data and measurement techniques through dedicated experiments. Among them, the shutdown dose rate (SDDR) measurement with a dosimetry system based on ion chambers for the validation of the numerical tools for the SDDR assessment in ITER, the on-line measurement of tritium production in the mock-up of the ITER HCPB-TBM (Helium Cooled Pebble Bed - Test Blanket Module) with a diamond detector to test some measurement systems capable of working in harsh environments as TBMs, and the first-of-a-kind experiment to measure the neutron-induced activation of cooling water in a tokamak during DT operation, to validate the multi-physics methodologies for water activation assessment in ITER. Moreover, as one of the main sources of radiological hazard in ITER is due to the Activated Corrosion Products (ACPs) circulating in the cooling system, an experiment is currently under design at the ENEA 14-MeV Frascati Neutron Generator (FNG) to prove the accuracy of the reference code in this matter for ITER (i.e., OSCAR-Fusion) under fusion relevant conditions. Finally, considering the importance of radiation-induced effects on electronics in ITER and future fusion machines, it is worth mentioning the development of a modular irradiation station at ENEA named GENeuSIS (General Experimental Neutron System Irradiation Station), to be installed at FNG and which aims at reproducing specific neutron and gamma energy spectra for studying the response of electronic devices and diagnostics.

The scope of the present work is to give an overview of the mentioned activities, mostly from an experimental point of view, to describe their status, achievements, criticalities emerged and the optimization of the next steps.

1. Introduction

Deuterium-Tritium (DT) campaigns at JET, culminated in the final DTE3 at the end of 2023, gave fundamental contributions for future fusion machines, primarily for ITER [1], including unique insights for the development of nuclear technology. The sub-project SP-5 [2] of the EUROfusion work package WP PrIO (Preparation of ITER Operations) [3], was established to continue the exploitation of the ITER-relevant radiation fields during DT campaigns at JET, earlier carried out within WP JET3 [4,5]. The aim is to improve the knowledge of nuclear technology and safety and to develop and validate nuclear codes, data and experimental techniques. Among the experiments carried out within WPPrIO SP-5 [2], the shutdown dose rate (SDDR) measurement with a dosimetry system based on ion chambers [6–11] for the validation of the numerical tools for the SDDR assessment in ITER, and the on-line measurement of tritium production in the mock-up of the ITER

* Corresponding author.
E-mail address: nicola.fonnesu@enea.it (N. Fonnesu).
[1] EUROfusion Consortium, JET, Culham Science Centre, Abingdon OX14 3DB, UK.

https://doi.org/10.1016/j.fusengdes.2025.115297
Received 17 January 2025; Received in revised form 25 May 2025; Accepted 23 June 2025
Available online 26 June 2025

HCPB-TBM (Helium Cooled Pebble Bed - Test Blanket Module) [12,13] with a diamond detector [14,15] to test some measurement systems capable of working in harsh environments as TBMs. Such experiments have been planned and refined since recent JET campaigns, including the second DT campaign (DTE2). A one-of-a-kind experiment (in a tokamak and under DT neutrons) was conducted for the first time during the third DT campaign (DTE3), to measure the neutron-induced activation of cooling water, to validate the multi-physics methodologies for water activation assessment in ITER [2,16]. Considering their ITER-relevance, it is worth mentioning also two experimental activities at the ENEA 14-MeV Frascati Neutron Generator (FNG), to support studies on Activated Corrosion Products (ACPs) and on the radiation-induced effects on electronics and diagnostics. In fact, ACPs circulating in the cooling system in ITER represent one of the main sources of radiological hazard and for this, an experimental hydraulic loop is currently under procurement at FNG, to prove the accuracy of the reference code in this matter for ITER (i.e., OSCAR-Fusion) under fusion and thermal hydraulics relevant conditions. Furthermore, considering the importance of Single Event Effects (SEE) on electronics in ITER and future fusion machines (in this regard, the experiment at JET during DTE3 is noteworthy [17]), a modular irradiation station named GENeuSIS (General Experimental Neutron System Irradiation Station) is under development. It aims at reproducing specific neutron and gamma energy spectra at FNG for studying the response of electronic devices and diagnostics.

Such activities are described in the following mostly from an experimental point of view. Their status, achievements, criticalities emerged, and the optimization of the next steps are highlighted. The manuscript is divided into two main sections: Section 2 is devoted to the experiments carried out at JET during DTE3, while Section 3 deals with the experiments planned at FNG. Finally, some concluding remarks and future work are given in Section 4.

2. Experiments at JET

The unique capability of JET to operate with the high-performance DT fuel mix was exploited across three experimental campaigns. The first one, DTE1, occurred in 1997 [18,19], while DTE2, in the second part of 2021, exploited the unprecedented ITER-relevant characteristics of the machine after the improvements post DTE1 [20]. DTE2 addressed several important physics and technological open points and achieved a new energy record in a single fusion plasma pulse (59 MJ). DTE3 occurred in the second part of 2023, from August 21st to October 14th, and demonstrated the controllability and reproducibility of high-power pulses carried out during DTE2 and set a new fusion energy record of 69 MJ achieved using advanced scenarios. Significant high neutron yield pulses were produced, up to $\sim 2.5 \times 10^{19}$ during record-breaking pulse #104522, with average neutron emission rate of $\sim 4.0 \times 10^{18}$ s^{-1} and a peak of $\sim 5.1 \times 10^{18}$ s^{-1}. From the nuclear technology standpoint, the importance of DTE3 is the significant 14-MeV neutron yield ($\sim 7.3 \times 10^{20}$) produced in an ITER-relevant machine as JET, from which the experimental activities in the following sub-sections benefited significantly.

2.1. Shutdown dose rate (SDDR)

The goal of measuring SDDR during inter-pulse periods and at the end of the JET experimental campaigns is to contribute to improve the accuracy of the simulation tools employed for shutdown dose rate predictions for ITER, as well as methodologies and nuclear data on which such numerical simulations are based. This is done through comparison of experimental data against numerical prediction and the analysis of discrepancy. A significant experimental dataset for benchmarking such numerical tools has been created since 2016 [6–10], at first across DD and TT campaigns (employed also to test and enhance the experimental setup, both from hardware and software standpoints), and then across DTE2 [11] and DTE3. SDDR is measured in air kerma rate, which is equivalent to absorbed dose rate under the condition of charged particle equilibrium [21].

The layout of the dosimetry system employed during DTE3 is sketched in Fig. 1(a). It is based on two air-vented ionization chambers (ICs), 1-liter volume and of spherical shape to limit the dependency of their response from the direction of the radiation field. ICs are installed ex-vessel, on dedicated shelves, by the horizontal ports of octant 1 (close to the Radial Neutron Camera) and octant 2 (above the ITER-like antenna). A detailed description of the components is given elsewhere for the setup of DTE2 [11]. With respect to that, during DTE3, the smaller IC earlier installed for higher dose rate in octant 1 was not employed. Instrument readout consists of two electrometers and a local computer (KN5A), located in J1D inside a dedicated cubicle. IC signal, i.e., ionization current whose range is roughly from some tens of fA to hundreds of pA, is transported from J1T to J1D through low-noise 100-meter long triaxial cables. Electrometers provide also high voltage (400 V) to the detectors. The piece of software for control, data acquisition, elaboration and sharing, was developed specifically for this purpose and refined across the JET campaign of the past. The interface with JET Control and Data Acquisition System (CODAS) is based on an exchange file as sketched in Fig. 1(b), to allow non-integrated software to access the JetFsm infrastructure in a file-based manner. SDDR data is sent to CODAS via HTTP protocol and made available in the Continuous Data Recording System (CGRT).

As for signal processing, the current I(t) measured by electrometers is integrated over a convenient time interval Δt and the resulting electric charge $Q(\Delta t)$, divided by the same time interval to get the average charge collected in the ionization chamber per unit of time ($Q/\Delta t$). Δt must be sufficiently long to limit statistical fluctuations of $Q/\Delta t$ and it was set equal to 30 s during DTE3. Once $Q/\Delta t$ is corrected to account for influence quantities, it is converted into air kerma rate by applying the calibration factor earlier measured at ENEA. Influence quantities considered are air conditions (pressure, temperature, humidity), since ICs are air-vented, ion recombination, stability, linearity, leakage current, direction of the radiation field, oxygen concentration into the air (during tritium operation oxygen concentration is reduced in J1T). Proper factors and uncertainties in their application are accounted in the uncertainty budget, according to the analysis detailed in [11] for DTE2. The same analysis of influence quantities and assessment of the experimental uncertainty is reasonably applicable also to DTE3 and the 1-sigma uncertainty related to the SDDR measurement is equal to 3.9 % and 4.2 %, respectively for ICs in octant 1 and 2. Probability density function is close to a Gaussian and the confidence probability of SDDR uncertainty is 64 and 66 %, respectively.

SDDR during the last two weeks of DTE3, as measured by the two dosimeters in octant 1 (IC Oct1 big) and octant 2 (IC Oct2 big), is shown in Fig. 1(c), bottom plot. The lower SDDR in the horizontal port of octant 2 is due to the presence of the ITER-like antenna, which contributes to the larger attenuation of gammas coming from the inner vessel with respect to octant 1, where the port is almost empty.

The upper plot in Fig. 1(c) is the neutron yield per pulse, on the same time axis as bottom plot. DD pulses at the end of October as tritium clean-up are visible as well. Different high-yield pulses were measured, some of them exceeding 10^{19} neutrons, thus producing a radiation environment extremely relevant for the aim of the experiment. SDDR level in octant 1 is ~300 μGy/h to some tens of mGy/h, in octant 2 is ~10 μGy/h to some hundreds of μGy/h and the selection of experimental points in such interval and across all DTE3 (during inter-pulses and at the shutdown) will contribute significantly to enrich the SDDR dataset for code benchmarking.

2.2. Test blanket module detector (TBMD)

Harsh conditions under which detectors for on-line measurement of radiation quantities (e.g., neutron and gamma flux, tritium production

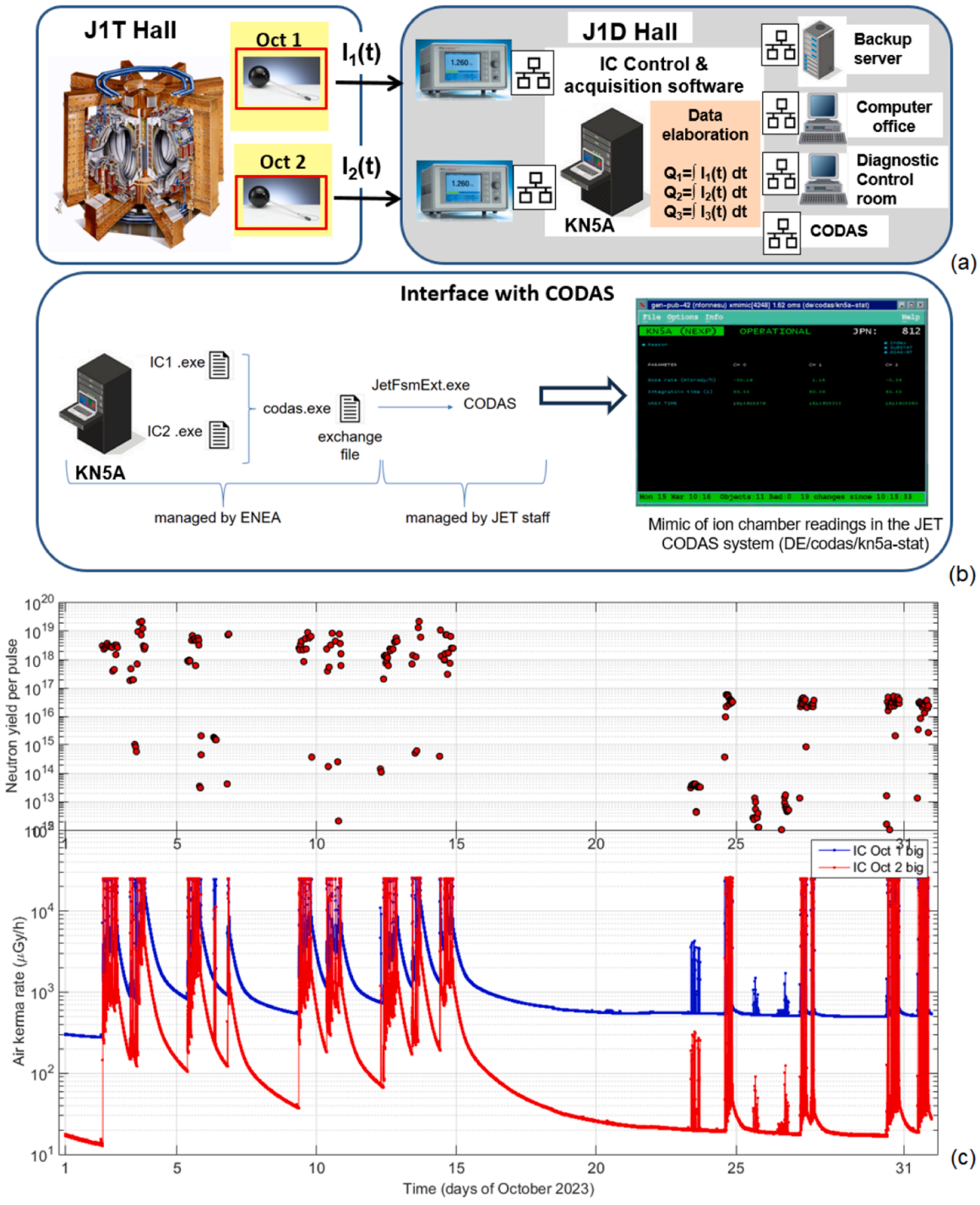

Fig. 1. (Color online) (a) Scheme of the software for dosimeter control, data acquisition and data sharing. (b) Interface with CODAS. (c) Neutron yield per pulse (top) and SDDR in μGy/h (bottom) in October 2023 during DTE3 (up to October 14th and DD clean-up in the second part of October) as measured by the two dosimeters in octant 1 (IC Oct1 big) and octant 2 (IC Oct2 big).

rate) are expected to work in ITER Test Blanket Modules (TBMs) impose proper testing and development. Within TBMD experiment, the mock-up of the HCPB TBM was located in the JET torus hall (J1T), on a dedicated support, near octant 8. A Single Crystal Diamond (SCD) detector with a ^{6}LiF coating to detect thermal neutrons through ^{6}Li(n,α)T reaction (detection is due to the energy released by 2.7-MeV tritons and 2.1-MeV alphas into the crystal bulk) was put inside the second (from plasma) of the four vertical channels of the mock-up to measure the tritium production. While the details of the calibration of the SCD detector are given elsewhere [14,15], here, for the sake of brevity, it is worth mentioning that the tritium production rate at the location of the detector is proportional to the counts per second (cps) measured by the detector (due to alphas and tritons) through the calibration coefficient measured at the thermal neutron flux density standard facility [22] of the Italian National Institute of Ionizing Radiation Metrology (INMRI) [23] of ENEA. The detector was exposed to DTE2 at first [15] and then, after some improvements, exposed to DTE3. During DTE2, it was observed that the measuring chain was not sufficiently fast to process detection events when the neutron emission rate was above ~10^{15} s^{-1}. The bottleneck, in terms of processing time, was the preamplifier, then

replaced (after DTE2). Noteworthy, the tritium production measured during some low-intensity pulses of DTE2, was $E = 1.40 \times 10^{-12}$ tritons per neutron source and the comparison against radiation transport calculation (C) gave a ratio $C/E = 0.77$ [15].

The layout of the detection system as during DTE3 campaign is sketched in Fig. 2(a). The mock-up is framed in the 3D view of octant 8 (upper-left). The 3D vertical section of the geometry model of the same mock-up (upper-right) shows the vertical channel where the detector is located. A low-noise charge amplifier Cividec Cx (type L) [24], installed in lieu of the preamplifier used during DTE2 and located some meters far from the SCD detector, is employed to amplify and shape signals. It ensures a high signal-to-noise ratio (SNR) at the multichannel analyzer (MCA) CAEN DT5780 [25] located in J1D, approximately 100 m far from the detector. High voltage (HV) is supplied by CAEN R1419ET [25], located in the same cubicle in J1D. The amplifier is equipped with a filter to suppress noise even from HV input and, with respect to the standard model Cx, type L is designed for longer cables and has improved SNR performance. A local computer, through some software specifically written by ENEA for the purpose, is employed to control data acquisition, to write measurement data in list-mode files, to store and backup data and to manage data sharing with CODAS. Since measurements are pulse-based, data acquisition is driven by trigger signals from JET UDP Server.

Some significant measurements across DTE3 are shown in Fig. 2(b), during pulses #104181, #104210 and #104213. The neutron emission rate across the plasma pulse measured by JET neutron monitor KN1 (light blue) and counts per second (cps) measured by the diamond detector (orange) are plotted on the same time axis to emphasize the overlapping and the good time agreement of neutron detection. Apparently, the limit in terms of neutron emission rate of plasma observed during DTE2 ($\sim 10^{15}$ s^{-1}) has been amply overcome thanks to the upgrade of the system, as confirmed by pulse #104213, during which TBMD system proved to be capable of working at a rate as high as 6×10^{16} s^{-1} without any interruption due to pile-up nor significant dead time. The maximum emission rate measured was $\sim 3 \times 10^{17}$ s^{-1} during pulse #104204, which means a neutron flux of $\sim 3 \times 10^{10}$ $cm^{-2}s^{-1}$ at the detector location. Above such a rate, the onset of measurement discontinuities is observed, likely caused by the communication between the digitizer and the local computer. In fact, the digitizer is equipped with USB 2.0 interface [25] that allows maximum data transfer rate up to 30 MB/s. Reasonably, it corresponds to the amount of data transferred at such count rate. A straightforward improvement could be employing an optical fiber interface, which would increase the transfer rate up to 80 MB/s. Finally, to convert cps into tritium production rate, after the upgrade of the measuring chain, a new calibration at the thermal neutron flux density standard facility is necessary.

As for extrapolation to ITER, the expected neutron flux in TBMs is approximately 500–1000 times the flux the SCD detector was exposed to ($\sim 3 \times 10^{10}$ $cm^{-2}s^{-1}$), during the most intense pulse measured (#104204). To adapt the detector to such higher flux, a viable way is the reduction of the detection efficiency through the reduction of the thickness of the LiF layer (thus limiting the conversion of neutrons into charge particles then detected into the crystal bulk) or by employing Li with natural isotopic abundance (7.5 % of Li6) instead of 95 % enriched in Li6 as the SCD detector. Moreover, the connection through optical fiber between digitizer and computer would allow to improve the maximum data transfer rate of almost 2.7 times. As for the hostile environment, since the mock-up is at room temperature, the effect of high temperature is not explored directly. A proper setup of detector assembly to limit leakage current in the connection cable between detector and amplifier is believed necessary, likely based on a mineral-insulted cable, as in earlier studies [26]. However, since the insulation material (e.g., alumina) at high temperature degrades, the leakage current in the cable may increase significantly (e.g., in alumina, w.r.t. room temperature, decrease of electric resistivity at 300 °C is so that leakage current increases by 4 orders of magnitude) and this aspect must be considered in the design of the cable.

2.3. Water activation (WACT)

The production of ^{16}N and ^{17}N through n,p reaction, respectively on ^{16}O and ^{17}O contained in water, is enabled under DT neutron irradiation, since both reactions have energy threshold below 14 MeV (10.2 and 8.4 MeV, respectively). As summarized in Table 1 (data from Ref. [27]), their subsequent β^- decay (again, into ^{16}O and ^{17}O, respectively), brings to the emission of high-energy gammas, especially from

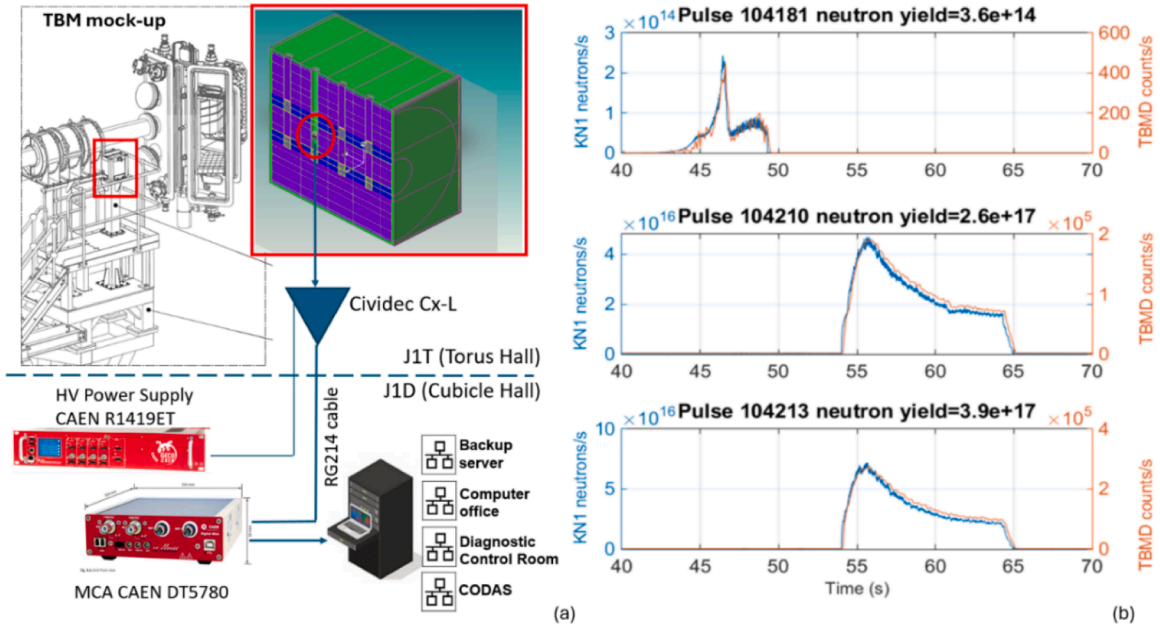

Fig. 2. (Color online) (a) Setup of the detection system at JET with detector and amplifier installed in the torus hall (J1T) and the rest of the measuring chain in the cubicle hall (J1D). (b) Neutron emission rate measured by KN1 monitor (light blue) and count rate of SCD detector across some JET pulses (orange) with increasing neutron yield (from top to bottom).

Table 1
Main gamma and delayed neutrons from decay of ^{16}N and ^{17}N (data from Ref. [27]).

Parent	Half-life (s)	Daughter	Type of Radiation	Energy (keV)	Absolute intensity %
^{16}N	7.13	^{16}O	Gamma	6128.6	67.0
				7115.1	4.9
^{17}N	4.17	^{17}O	Gamma	870.7	3.1
		^{16}O	Delayed Neutrons	387.0	35.8
				886.0	0.5
				1163.0	47.6
				1690.0	7.0

^{16}O (6.1 and 7.1 MeV), while part of the ^{17}O decays further into ^{16}O through the emission of delayed neutrons (the majority being emitted at 0.4 and 1.2 MeV).

Despite short-lived, considering typical speed of water in cooling loops (from a few to about ten meters per second), such movable radiation sources may be transported quite far from the birth place, thus causing additional nuclear heating onto components along the way (the case of superconducting magnets is critical), and, outside the biological shield, radiation exposure for workers and relevant dose rate for electronics and radiation-sensitive devices. While ^{16}N is the dominant nuclide during plasma operation, mainly with emission of gammas at 6.1 and 7.1 MeV, delayed neutrons from ^{17}N are responsible for activation of pipework with longer lasting effects after shutdown [28,29], with implications on SDDR and maintenance plan.

It is therefore clear the importance of accurate modeling of such movable radiation sources and their transport. DTE3 offered the possibility to build a unique dataset for the validation and further development of numerical tools and methodologies used for assessing water activation in ITER (which basically couple fluid dynamics, radiation decay and transport), and even to explore diagnostic systems for such a kind of measurements.

The water loop of the Neutral Injector Box (NIB) was taken as case study since compliant with the requirements of the WACT experiment and NIB of octant 4 was preferred to the one of octant 8 as more suitable [2]. The measurement section selected, shown in Fig. 3(a), is in the basement below NIB of octant 4 and it is the collector horizontal pipeline in which duct scraper and RHVV (i.e., Rotary High Vacuum Valve, connects the NIB and the Torus Vacuum Vessel) cooling lines merge. To measure the gamma energy spectrum of the activated water flowing through the horizontal pipe, two scintillators (3″x3” crystal size sodium iodide doped with thallium, or NaI, and bismuth germanate, or BGO) with photomultiplier tube (PMT), have been located below the tube, in a position sufficiently far from the merging points of the two vertical cooling lines, to guarantee the two flows coming from duct scraper and RHVV are fully mixed at the measurement section. BGO and NaI, equipped with proper lead shielding (5-cm thick chevron bricks) and collimators (to adjust detection efficiency depending on the plasma neutron yield), were located on a support of aluminum. On top, an ion chamber 1-liter volume, same model as SDDR experiment (cfr. Sub-Section 2.1) was installed to measure dose rate but not operated as the transmission cable (not the original one, due to fire safety prescriptions) connecting to the electrometer in J1D, was found not compatible for transmission of such a small current during tests. In the same Fig. 3(a), the frame for calibration with standard gamma sources is visible. They are a mixed nuclide source (which includes ^{137}Cs, ^{88}Y and ^{60}Co), a ^{60}Co source and a $^{244}Cm/^{13}C$ source [16]. The latter emits 6.1 MeV gammas (due to ^{16}O resulting from α,n reaction on ^{13}C) and allows to have an energy-calibration point also at this energy.

WACT measurements started during the DD campaign (C45) preceding DTE3, also employed to test and refine tuning of the experimental setup and acquisition parameters, and continued also across clean-up (C47) and the long-pulse section in DD. The main outcomes of WACT measurements are in [2].

The rest of the experimental setup was in J1D, cubicle KM8, as shown in Fig. 3(b). The high-voltage power supply modules (Ortec 556) were employed to bias PMTs (final settings were −650 V for NaI and 1400 V for BGO).

Detection signals from PMTs were digitized using a CAEN DT5730B device, connected to a computer and controlled by a customized software developed by ENEA to control data acquisition in list-mode (to get the energy spectra in specific time intervals with respect to the JET pulse, since the activated water flow is expected at the measurement section with some delay), to store and backup data and to manage data sharing with CODAS. As for TBMD, data acquisition is triggered by signals from JET UDP Server, but in this case the end of acquisition accounts for the transit time of water up to the measurement section.

While WACT measurements were carried out across > 1500 plasma pulses with BGO, the detection rate of NaI was too high for the system and the excessive number of pile-up events prevented from having a full dataset of measurements. Unlike the PMT of BGO, the PMT of NaI is non-compensated and the high count rate, which turns into a high anode current, is suspected to be the cause of significant gain drift. The problem was in part mitigated by lowering the magnitude of voltage bias (−650 V is the final setting) and by employing an algorithm for pile-up rejection available in the commercial data acquisition software CoMPASS [25] and non-implementable in the ENEA acquisition software. For this, a parallel acquisition chain was made with a second digitizer

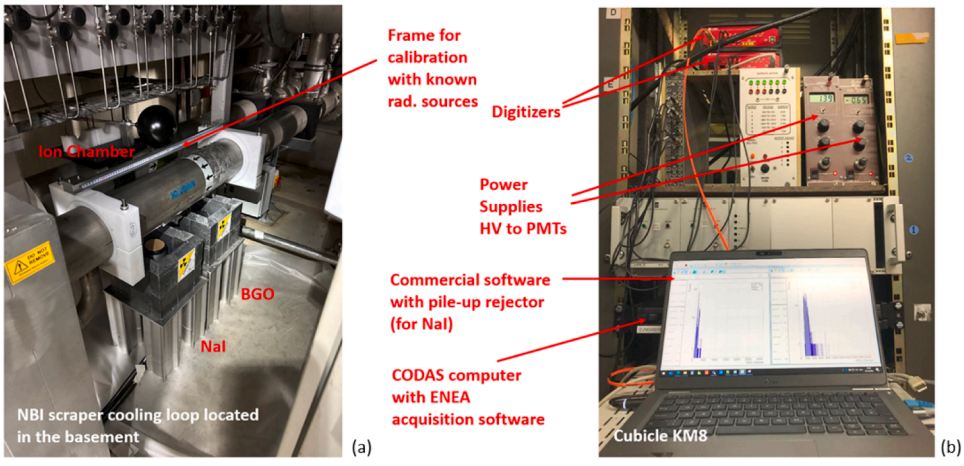

Fig. 3. (a) Picture of basement below JET Neutral Injector Box (NIB) of octant 4 and horizontal pipe which collects cooling lines from duct scraper and RHVV and experimental setup of the detection system to measure water activation. (b) Cubicle KM8 in J1D with measurement chain of WACT experiment.

controlled by CoMPASS, as visible in Fig. 3(b), connected to a computer with an optical fiber link to improve the transfer rate. The acquisition was triggered manually during the last days of DTE3, more precisely from October 2nd to 9th. Data acquisition was performed in the so-called wave mode, during which the time evolution of each detection pulse is recorded, thus allowing possibly the correction of pile-up events not rejected through the development of a post-analysis algorithm. Some more NaI measurements were carried out during the JET long-pulse section in DD at the end of November. In total, ~30 gamma energy spectra were measured by NaI.

While the characteristics of the dataset in terms of operation conditions explored (i.e., neutron yield range >5 orders of magnitude and neutron emission up to 60 s) are given elsewhere [2], here an example of WACT measurements with BGO is given during DD pulse #104074, pre-DTE3. In Fig. 4(a) total neutron emission rate measured by JET monitor KN1 (DT neutrons are ~1 % of the total) and BGO count rate are plotted on the same time axis and the BGO count rate peak after $t = 50$ s is due to activated water flowing at the measurement section. By selecting only detection events after plasma pulse, the energy spectrum binned with 1000 channels shows the peaks at 6.1 and 7.1 MeV due to ^{16}N, Fig. 4(c).

3. Experiments at the frascati neutron generator (FNG)

FNG [30] is a 14-MeV accelerator-driven neutron source based on a duoplasmatron ion source and linear electrostatic accelerator in which up to 1 mA positive deuterium ions (D^+) are accelerated up to 300 keV against a tritiated titanium target. It has been operating since 1992 providing a neutron source strength up to 1.5×10^{11} s^{-1} in support of relevant fusion neutronics experiments. Among the most relevant activities carried out, benchmark experiments of relevance for ITER, contribution to primary neutronics benchmark databases and nuclear data are noteworthy. Development and test of neutron detectors and other diagnostics for fusion experiments are relevant as well. Another trending topic is the characterization and test of electronics under neutron irradiation for fusion. In line with its mission, two experiments in support of ITER are currently under development as detailed in the following sub-sections.

3.1. Water loop for ACP

Inside the cooling loops of high-performance fusion facilities as ITER, the water-wall interaction causes corrosion, erosion and subsequent release of the so-called corrosion products, which get activated under intense neutron irradiation produced by plasma. Activated corrosion products (ACPs) represent a moving and intense radiation gamma source exiting the conventional radiation shielding of the tokamaks through cooling loops and they are a concern in terms of occupational radiation exposure (ORE) during maintenance and in case of severe accidents involving loss of coolant.

The accurate and reliable modeling of the generation, transport and deposition of ACPs, and the subsequent calculation of the activity in cooling loops of high-performance fusion facilities as ITER, is a critical safety concern. Existing codes to perform such modeling are derived from fission and a significant benchmark effort is needed to check their reliability in fusion facilities, where, with respect to fission, the neutron radiation field, structural materials and thermal-hydraulic characteristics of water flow in cooling loops vary significantly. Currently, the reference code for the ACPs assessment in the ITER framework is OSCAR-Fusion [31].

As anticipated, experimental validations are available mainly in fission conditions and this requires the design of dedicated experiments under fusion-relevant conditions. Among the experiments devoted to this, within the EUROfusion WP PrIO, a task of SP-5 aims at realizing a hydraulic loop at FNG to study ACPs under thermo-hydraulic, chemical and neutronic conditions relevant for ITER. The hydraulic loop shall be installed at ENEA Frascati in the FNG building, inside the hall adjacent to the experimental hall of the neutron source.

ACPs are in two forms, i.e., ions and solid particles, and their study will occur through experimental campaigns to validate and refine the main mechanisms which influence their transport in the cooling loops of ITER and simulated by OSCAR-Fusion. The OSCAR-Fusion models which will be explored in the loop at FNG include dissolution and precipitation of ions, fluid-dynamics transport and purification of ions and particles and the deposition of particles. Considering the working hours necessary to produce enough corrosion products in the loop, corrosion and erosion are not included among the mechanisms studied at FNG and CPs will be

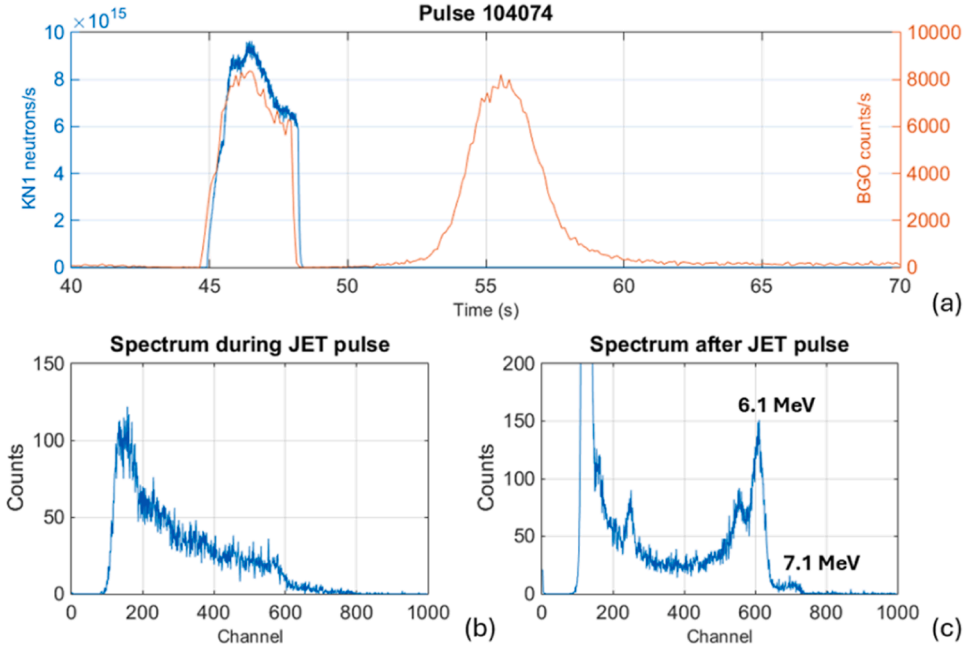

Fig. 4. (a) Neutron emission rate measured by KN1 monitor (light blue) and count rate of BGO across JET pulse #104074. (b) BGO gamma energy spectrum during the plasma pulse and (c) after the pulse with the indication of 6.1 and 7.1 MeV gamma peaks due to ^{16}N decay.

injected in the form of activated ions and solid particles in a dedicated section of the same hydraulic loop (cfr. Fig. 5). Noteworthy, the code allows to simulate direct injection of CPs. As for corrosion and erosion mechanisms, dedicated experiments are ongoing and planned in the near future, especially for CuCrZr for which such mechanisms are not properly modeled at the conditions relevant for fusion. In this regard, some CuCrZr samples were recently exposed at water reducing conditions (240 °C, 45 bar, $O_2 < 10$ ppb) inside an autoclave at RINA labs. to measure corrosion rate [32]. After installation and testing, the prosecution of the task implies the design of experimental campaigns to study specific gamma-emitters relevant for ITER under the form of solid particles and ions. CPs will be activated through 14-MeV neutron irradiation at FNG, then injected into the loop and their activity measured in the measurement sections (cfr. Fig. 5). Measurements, in terms of activity (per unit of water volume and per unit of pipe surface) will be then compared against OSCAR-Fusion predictions.

The main water parameters to be achieved in the hydraulic loop are given in Table 2 and the relevancy for ITER case is confirmed by comparison with typical water conditions expected in the ITER IBED (Integrated Blanket, Edge Localized Mode/Vertical Stability, and Divertor) Primary Heat Transfer System (PHTS) during plasma operation of the tokamak, i.e., water temperature = 150 °C, velocity = 10 m/s, Reynolds number = 10^6–10^7, water pH_T =7 and O_2 content = 10 ppb. A scheme of the hydraulic loop in the form of Piping and Instrumentation Diagram (P&ID) in Fig. 5, as a compromise resulting from scientific needs, safety and compatibility with FNG facilities, market survey to explore the availability of the components and time schedule for procurement.

Thermodynamic water conditions being 140 °C and 6 bar, the components must be compliant with the European Pressure Equipment Directive (PED 2014/68/UE). The main parts of the loop shown in Fig. 5 are described in the following.

The water expansion tank proposed is a 10-liter volume, maximum water temperature 120 °C, made of steel AISI 304. Its function, besides limiting the effect of water expansion, is to supply water to the loop, to set the pressure in the loop at the connection point with the same. A heat sink is foreseen to connect the tank to the loop to cool down water from 140 °C to 120 °C in case of reverse flow. The tank is equipped with a pressure relief device which vents into the hall, if necessary, to limit overpressure. Water temperature and water level inside the tank are measured and sent to the central control system. Pressure inside the tank is controlled through nitrogen inflation. A nitrogen tank is connected through the gas line shown in Fig. 5. Inflation of nitrogen into the loop is employed also to lower and keep the oxygen concentration at the content needed for the experiment (cfr. Table 2).

Table 2
Water parameters and characteristics of the loop.

Parameter	Quality/quantity
Water type	Demineralized water
Nominal Temperature and Pressure	140 °C, 6 bar
Maximum Volumetric Flow Rate	Approx. 80 l/min
Nominal Volumetric Flow Rate	Approx. 60 l/min
Maximum water speed	Approx. 15 m/s
Linear length of the loop	Approx. 20 m
Water volume	Approx. 20 l
Water velocity range	3–13 m/s
Reynolds number range	$5 \times 10^4 - 5 \times 10^5$
Oxygen content into the water	10–100 ppb
pH_T of water	

As for pumping and heating unit, it is proposed a commercial system [33], 10 kW of total power and 140 °C nominal water temperature. The unit is compliant with the electric grid of FNG building (3-phase socket, 16 A, 380 V). Each phase powers a 3-kW electric resistance for a total heating power available of 9 kW. The centrifugal pump is 1 kW power, flow rate range 20–80 l/min, pump head 33 m (@20 l/min) and 27 m (@80 l/min). It can operate at full temperature of 140 °C thus avoiding the installation of a chiller upstream on the same pump. Temperature is controlled by a PID controller, within ±0.5 °C. The unit is also equipped with a 5-liter expansion tank and safety shutdown in case nominal pressure and temperature are exceeded. A bypass loop which connects pump outlet to the inlet, allows to vary the flow rate into the main loop by recirculating a fraction of the flow.

Concerning piping, it is proposed type PN16 (i.e., maximum pressure 16 bar at 20 °C), made of stainless steel SS316L, 18 mm diameter, 1 mm thick (to be confirmed). Type 22 diameter, 1.2 mm thick, is still an option to reduce the maximum water velocity, if needed. As for rugosity,

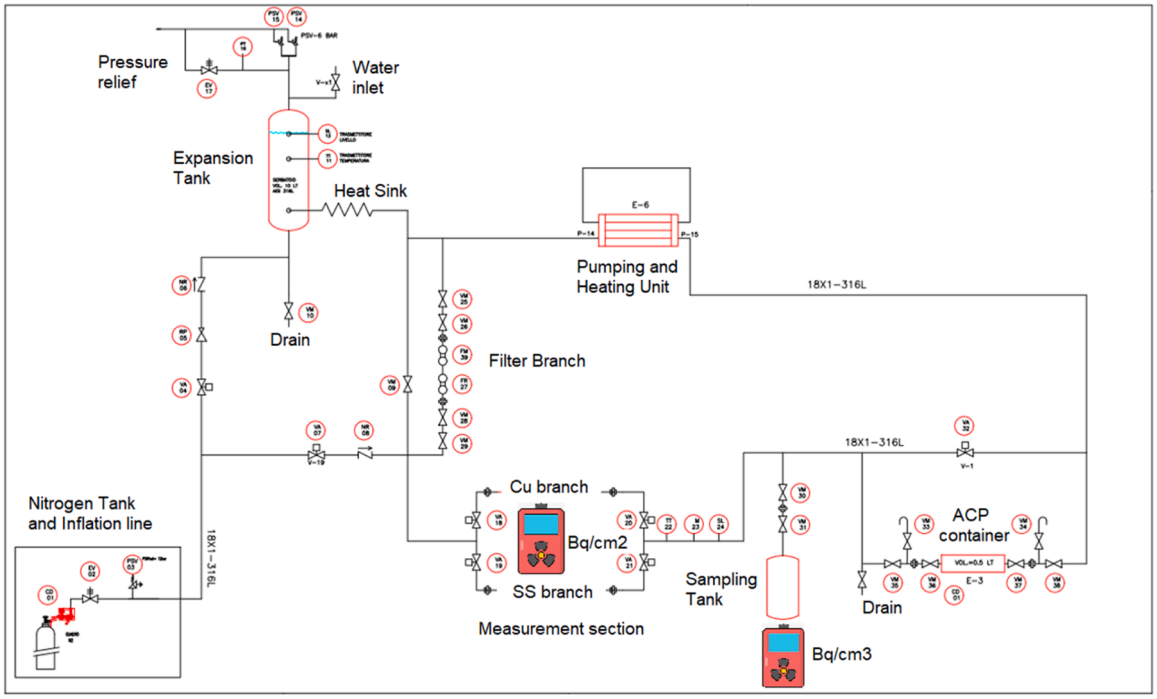

Fig. 5. Diagram of ACP loop at FNG.

the manufacturer reported Ra = (0.50 ± 0.20) μm.

The radiation measurement section is the part of the loop where radiation detectors shall be installed, close to the pipes, to measure the gamma radiation activity per unit of pipe surface, one of the main OSCAR-Fusion outputs. It is proposed to employ portable High Purity Germanium (HPGe) detectors to accurately identify radionuclides and to perform spectrometry, equipped with proper collimators to focus the measurement at specific points along the pipes. Such section of the loop is made of two 2-meter-long parallel branches, one is made of copper and one in SS316L, pipes 12 mm diameter, 1 mm thick. Since rugosity is one of the parameters of influence of ACPs transport and change of rugosity is relevant for the experiment, the first half of the two lines has Ra =0.50 μm and the latter Ra =10–15 μm. The two branches are equipped with shut-off valves as the experiments foresee the alternating use of them.

Solid particles or ions injected into the loop must be filtered at the end of each experiment through a filtering system. For this, a branch with two filters in series to be open during cleaning phase of water, is foreseen. It is proposed to install a water filter based on 10″ cartridge of Polypropylene, 1-μm filtration, in addition to a water filter based on mixed bed resin cartridge. Double shut-off valves are requested on the filtering branch.

ACPs to be injected into the loop are initially contained in a cylindrical holder, 0.5-liter volume, preferably made of aluminum (to limit neutron activation of the same). Upstream and downstream the container, a vent valve is placed between two shut-off valves to vent out oxygen accumulated during the installation of the same holder into the loop.

To sample water for measuring the activity per unit of volume, another relevant output of OSCAR-Fusion, a 0.5-liter volume cylindrical container, preferably made of aluminum, is to be installed at the end of the sampling line. It is foreseen to perform the measurement of activity of sampled water with the well-type HPGe of FNG laboratory.

As for monitoring of the loop, some probes to measure water temperature, pressure and flow rate (electromagnetic flow meter) at the radiation measurement section are foreseen. Such quantities are also relevant parameters to be considered in OSCAR-Fusion simulations, so it is important to have an accurate and real-time measurement of them. Water temperature, pressure and level will be measured also in the expansion tank. A central control system will acquire such measurements and will allow the control of electric valves.

3.2. GENeuSIS (General experimental neutron system irradiation station)

Radiation-induced effects on electronics in high-power fusion machines as ITER, can be destructive as the ones due to accumulated radiation dose or non-destructive and probabilistic, as the ones caused by interaction with single energetic particles including fusion neutrons (Single Event Effect or SEE), which normally appear as transient pulses in logic or support circuitry, or as the switching of a bit value (bitflips) in memory cells or registers [34,35]. They may lead to the failure of the electronic device thus representing serious concern especially if it is part of a critical system. Strategies of mitigation of exposure and radiation hardening are important but, in any case, proper measurement of performance and testing under fusion relevant radiation field is necessary. In this regard, it is worth mentioning the recent experiment at JET under DTE3 [17]. Neutron sources as FNG cannot directly reproduce the complex radiation energy spectra as the ones to which the electronic components are exposed in fusion machines and for this, the GENeuSIS project was proposed by ENEA. The aim is designing and manufacturing proper modular assemblies with a layer structure of moderator materials to be located in front of the 14-MeV neutron source of FNG, to reproduce neutron and gamma (the latter by adding embedded gamma sources) energy spectra as expected in locations in which components or systems of interest will be installed in ITER. In parallel, a supervised machine learning model to support the design of the assemblies to have specific radiation energy spectra inside the test cavity, is under development [36]. Among the cases studied so far, there are two 60 × 80 × 60 cm^3 assemblies with a 20 × 30 × 20 cm^3 test cavity, inside which the neutron energy spectrum as expected in two locations of the diagnostic Equatorial Port #12 (Port Interspace and Port Cell), are reproduced. The first assembly, to reproduce the spectrum in the Port Interspace (GENeuSIS-I) is made of Cu, Pb, Cd, SS and Perspex, while the second one, to reproduce the spectrum in the Port Cell (GENeuSIS-II), is made of Cu, an alloy of W (densimet), Pb, SS, Perspex, Teflon and Cd.

While optimization is in progress, preliminary results are quite promising as they show good reproducibility, both for GENeuSIS-I and GENeuSIS-II. The assembly of GENeuSIS-II is shown in Fig. 6(a) and the comparison between normalized neutron flux energy spectrum as in ITER port cell and as expected in the test cavity is given in Fig. 6(b). Besides the close reproduction of the neutron flux energy spectrum, simulations show that the same total neutron flux as in the location in the ITER Port Cell (i.e., 5.6 × 10^5 $cm^{-2}s^{-1}$) can be obtained at FNG inside test cavity of GENeuSIS-II with a neutron strength of ~5 × 10^9 s^{-1}, an intensity at which the neutron source is routinely operated.

4. Remarks and future work

DT campaigns at JET, culminated in DTE3, represented a unique chance to improve the knowledge of nuclear technology and safety and to develop and validate nuclear codes, data and measurement techniques through dedicated experiments of relevance for ITER. From the nuclear technology standpoint, the importance of the final DTE3 campaign is the significant 14-MeV neutron yield (~7.3 × 10^{20}) produced in an ITER-relevant machine as JET and among the activities which benefited from that within WP PrIO SP-5, there are the SDDR, TBMD and WACT experiments.

A dosimetry system installed in the JET Torus Hall has provided a large set of data for SDDR code benchmarking since 2016 and the past campaigns (DD and TT) have been exploited also to refine the measurement system, both hardware and software, in preparation of the subsequent DT campaigns. High-yield pulses during DTE3, some of them exceeding 10^{19} neutrons, produced a radiation environment extremely relevant for the aim of the experiment, and the selection of experimental points during inter-pulses and at the shutdown will contribute significantly to enrich the SDDR dataset for code benchmarking. Collecting SDDR data, as long as possible, across the final JET shutdown and during decommissioning, is important since never done before in a tokamak machine of such importance.

As for TBMD for testing detector for ITER TBMs under fusion relevant operating conditions, the limit of neutron emission rate of plasma observed during DTE2 (~10^{15} s^{-1}) has been amply overcome during DTE3 after the upgrade of the system, as confirmed by pulse #104213, during which TBMD system proved to be capable of working at a rate as high as 6 × 10^{16} s^{-1} without any interruption due to pile-up nor significant dead time. The maximum emission rate measured was ~3 × 10^{17} s^{-1} during pulse #104204, which means a neutron flux of ~3 × 10^{10} $cm^{-2}s^{-1}$ at the detector location. Above such a rate, the onset of measurement discontinuities is observed, likely caused by the communication between digitizer and the local computer and this limit can be overcome through optical fiber link.

WACT, the first-of-a-kind experiment to measure the neutron-induced activation of cooling water in a tokamak during DT operation to validate the multi-physics methodologies for water activation assessment in ITER, produced a dataset of ~1500 pulses with BGO and ~30 pulses with NaI detectors, in a wide range of operation conditions in terms of neutron yield and plasma pulse length. Such a relevant dataset will be made available for code benchmarking.

In addition, two relevant projects of interest for ITER are under development at the ENEA 14-MeV Frascati Neutron Generator, to study ACPs (one of the main sources of radiological hazard for workers) in a hydraulic loop, and to produce irradiation stations (GENeuSIS) to

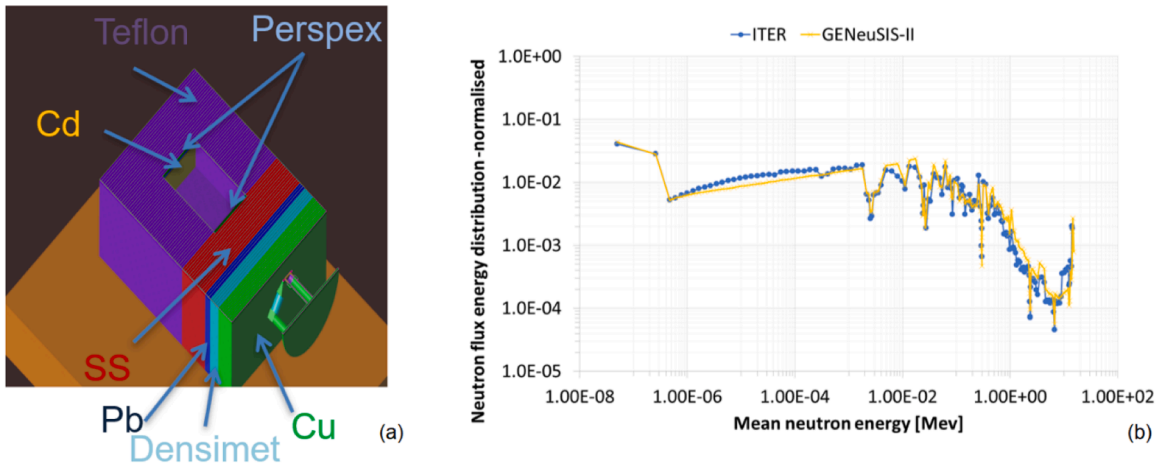

Fig. 6. (Color online) (a) GENeuSIS II assembly and (b) comparison between normalized neutron flux energy spectrum as in ITER port cell and as expected in the test cavity.

replicate specific radiation fields in terms of energy flux spectrum, mainly to test electronics against radiation-induced effects.

The hydraulic loop has been designed and engineered to study ACPs under thermo-hydraulic, chemical and neutronic conditions relevant for ITER at FNG, accounting scientific needs, safety and compatibility with the laboratory, availability of components on the market and time schedule of the project. It is currently under procurement, and, after installation and testing, experimental campaigns will be planned to study specific corrosion products. These corrosion products will be activated through 14 MeV neutron irradiation and then injected into the loop to investigate the main mechanisms influencing their transport in the cooling loops of ITER. They will be simulated with OSCAR-Fusion to compare measurements against predictions.

Finally, among the irradiation stations proposed within GENeuSIS project, two assemblies with test cavity, inside which the neutron energy spectrum as expected in Port Interspace and Port Cell of Equatorial Port #12 is replicated, are under development. While optimization is in progress, preliminary results show quite close agreement with the reference neutron flux energy spectra in both cases.

CRediT authorship contribution statement

N. Fonnesu: Writing – original draft, Supervision, Methodology, Investigation, Formal analysis, Data curation, Conceptualization. **P. Beaumont:** Methodology, Investigation. **T. Berry:** Validation, Formal analysis. **A. Colangeli:** Writing – review & editing, Methodology. **F. Dacquait:** Investigation, Formal analysis. **M. Damiano:** Investigation, Formal analysis. **D. Flammini:** Writing – review & editing, Methodology. **C.L. Grove:** Validation, Formal analysis. **X. Litaudon:** Supervision, Resources, Project administration. **S. Loreti:** Software, Methodology, Investigation, Data curation, Conceptualization. **M. Lungaroni:** Writing – review & editing. **S. Mianowski:** Methodology, Investigation. **F. Moro:** Writing – review & editing, Software. **S. Noce:** Methodology, Investigation, Formal analysis, Conceptualization. **J. Peric:** Methodology, Investigation, Formal analysis. **A. Previti:** Writing – review & editing, Methodology. **V. Radulović:** Methodology, Investigation, Formal analysis, Conceptualization. **R. Villari:** Supervision, Project administration, Methodology, Formal analysis, Conceptualization. **P. Zito:** Writing – review & editing, Project administration, Investigation.

Declaration of competing interest

The authors declare the following financial interests/personal relationships which may be considered as potential competing interests:

Nicola Fonnesu reports financial support was provided by European Consortium for the Development of Fusion Energy. If there are other authors, they declare that they have no known competing financial interests or personal relationships that could have appeared to influence the work reported in this paper.

Acknowledgments

This work has been carried out within the framework of the EUROfusion Consortium, funded by the European Union via the Euratom Research and Training Programme (Grant Agreement No 101052200 — EUROfusion). Views and opinions expressed are however those of the author(s) only and do not necessarily reflect those of the European Union or the European Commission. Neither the European Union nor the European Commission can be held responsible for them.

Data availability

Data will be made available on request.

References

[1] C.F. Maggi, et al., Overview of T and D-T results in JET with ITER-like wall, Nucl. Fusion 64 (2024) 112012, https://doi.org/10.1088/1741-4326/ad3e16.
[2] R. Villari, et al., Overview of deuterium-tritium nuclear operations at JET, Fusion Eng. Des. 217 (2025) 115133, https://doi.org/10.1016/j.fusengdes.2025.115133.
[3] X. Litaudon, et al., Eurofusion contributions to ITER nuclear operation, Nucl. Fusion 64 (2024) 112006, https://doi.org/10.1088/1741-4326/ad346e.
[4] P. Batistoni, et al., Technological exploitation of deuterium–Tritium operations at JET in support of ITER design, operation and safety, Fusion Eng. Des. 109-111 (2016) 278–285, https://doi.org/10.1016/j.fusengdes.2016.03.012.
[5] R. Villari, et al., Neutronics experiments and analyses in preparation of DT operations at JET, Fusion Eng. Des. 109 (2016) 895–905.
[6] R. Villari, et al., ITER oriented neutronics benchmark experiments on neutron streaming and shutdown dose rate at JET, Fusion Eng. Des. 123 (November 2017) 171–176, https://doi.org/10.1016/j.fusengdes.2017.03.037.
[7] N. Fonnesu, et al., The preparation of the shutdown dose rate experiment for the next JET deuterium-tritium campaign, Fusion Eng. Des. 123 (November 2017) 1039–1043, https://doi.org/10.1016/j.fusengdes.2017.01.030.
[8] N. Fonnesu, et al., Shutdown dose rate measurements after the 2016 deuterium-deuterium campaign at JET, Fusion Eng. Des. 136 (Part B) (November 2018) 1348–1353, https://doi.org/10.1016/j.fusengdes.2018.05.006.
[9] N. Fonnesu, et al., Shutdown dose rate studies for the DTE2 campaign at JET, Fusion Eng. Des. 161 (December 2020) 112009, https://doi.org/10.1016/j.fusengdes.2020.112009.
[10] N. Fonnesu, et al., Dose rate measurements during the tritium campaign at JET and diagnostic improvements for the deuterium–Tritium experiments, IEEE Trans. Plasma Sci. 50 (11) (Nov. 2022) 4131–4137, https://doi.org/10.1109/TPS.2022.3169631.
[11] N. Fonnesu, et al., Shutdown dose rate experiment at JET during DTE2, Eur. Phys. J. Plus 139 (2024) 432, https://doi.org/10.1140/epjp/s13360-024-05208-w.
[12] P. Batistoni, et al., Neutronics experiment on a helium cooled pebble bed (HCPB) breeder blanket mock-up, Fusion Eng. Des. 82 (2007) 2095–2104, https://doi.org/10.1016/j.fusengdes.2007.04.009.

[13] P. Batistoni, et al., Neutronics experiments for uncertainty assessment of tritium breeding in HCPB and HCLL blanket mock-ups irradiated with 14 MeV neutrons, Nucl. Fusion 52 (2012) 083014, https://doi.org/10.1088/0029-5515/52/8/083014.
[14] M. Angelone, et al., Calibration and test of a 6LiF-diamond detector for the HCPB mock-up experiment at JET, Fusion Eng. Des. 146 (2019) 1755–1758.
[15] N. Fonnesu, et al., Measurement of tritium production in the helium cooled pebble bed test blanket module mock-up at JET during DTE2, Eur. Phys. J. Plus 139 (2024) 893, https://doi.org/10.1140/epjp/s13360-024-05670-6.
[16] V. Radulovic, et al., Preparation of a water activation experiment at JET to support ITER, Fusion Eng. Des. 169 (2021) 112410, https://doi.org/10.1016/j.fusengdes.2021.112410.
[17] M. Dentan, et al., in: Real-Time SER measurements of cmOS Bulk 40 nm and 65 nm SRAMs combined with neutron spectrometry at the JET Tokamak during D-D and D-T plasma operation, NSREC 2024 - 2024 IEEE Nuclear and Space Radiation Effects Conference, Ottawa, Canada, Jul 2024.
[18] M. Keilhacker, et al., High fusion performance from deuterium-tritium plasmas in JET, Nucl. Fusion 39 (1999) 209, https://doi.org/10.1088/0029-5515/39/2/306.
[19] J. Jacquinot, et al., Overview of ITER physics deuterium-tritium experiments in JET, Nucl. Fusion 39 (1999) 235, https://doi.org/10.1088/0029-5515/39/2/307.
[20] J. Mailloux, et al., Overview of JET results for optimising ITER operation, Nucl. Fusion 62 (2022) 042026, https://doi.org/10.1088/1741-4326/ac47b4.
[21] International Commission on Radiation Units and Measurements (ICRU), fundamental quantities and units for ionizing radiation, J. ICRU 11 (1) (2011). Report 85.
[22] E. Rotondi, et al., Thermal neutron flux density standard at C.S.N. Casaccia: design and calibration, Energ. Nucl. 21 (1) (1974) 53–55.
[23] https://www.inmri.enea.it/en/metrology, Internet site accessed in November 2024.
[24] Cividec, https://cividec.at/electronics-Cx-L.html, Internet site accessed in November 2024.
[25] CAEN, https://www.caen.it, Internet site accessed in November 2024.
[26] M. Angelone, et al., Properties of diamond-based neutron detectors operated in harsh environments, J. Nucl. Eng. 2 (4) (2021) 422–470, https://doi.org/10.3390/jne2040032.
[27] https://www-nds.iaea.org/relnsd/vcharthtml/VChartHTML.html, Internet site Nuclear data services IAEA, accessed in November 2024.
[28] Z. Ghani, et al., Radiation levels in the ITER tokamak complex during and after plasma operation, Fusion Eng. Des. 96–97 (October) (2015) 261–264.
[29] S. Jakhar, M. Loughlin, Calculation of activation water radiation maps in ITER, neutronics challenges of fusion facilities – II, in: Transactions of the American Nuclear Society, San Francisco, California 116, 2017. . June 11–15.
[30] M. Martone, et al., The 14 MeV Frascati neutron generator, J. Nucl. Mater. 212–215 (Part B) (September 1994) 1661–1664, https://doi.org/10.1016/0022-3115(94)91109-6.
[31] F. Dacquait, et al., Modelling of the contamination transfer in nuclear reactors: the OSCAR code - applications to SFR and ITER, in: 1st IAEA Workshop on Challenges for Coolants in Fast Neutron Spectrum Systems, Vienne, Austria, Jul 2017.
[32] S. Noce, et al., Experimental tests for the characterization of corrosion behavior of CuCrZr under ITER baking conditions. submitted to the Special Issue of the 33rd Symposium on Fusion Technology (SOFT), Dublin, 2024.
[33] https://www.tempco.it, Internet site accessed in November 2024.
[34] https://radhome.gsfc.nasa.gov/radhome/see.htm, Internet site accessed in November 2024.
[35] G.C. Messenger, M.S. Ash, Single event phenomena I. Single Event Phenomena, Springer, Boston, MA, 1997, https://doi.org/10.1007/978-1-4615-6043-2_6.
[36] M. Damiano, et al., Preliminary study for a machine learning model for GENeuSIS. submitted to the Special Issue of the 33rd Symposium on Fusion Technology (SOFT), Dublin, 2024.